Can the toxicity of polyethylene microplastics and engineered nanoclays be influenced by the presence of each other? The flatfish Solea senegalensis larvae as a case study

Lígia M.B.M. Santana[1,2], Andreia C.M. Rodrigues[3], Diana Campos[3], Olga Kaczerewska[4], Joana Figueiredo[1], Sara Silva[1], Isabel Sousa[4], Frederico Maia[5], João Tedim[4], Denis M.S. Abessa[2], Pedro Pousão-Ferreira[6], Ana Candeias-Mendes[6], Florbela Soares[6], Sara Castanho[6], Amadeu M.V.M. Soares[3], Rui J. M. Rocha[3], Carlos Gravato[7], Ana L. Patrício Silva[3*], Roberto Martins[3]

[1] Department of Biology, University of Aveiro, 3810-193 Aveiro, Portugal
[2] Campus do Litoral Paulista, Universidade Estadual Paulista (UNESP), 11330-900 - São Vicente, SP, Brazil
[3] CESAM-Centre for Environmental and Marine Studies and Department of Biology, University of Aveiro, 3810-193 Aveiro, Portugal
[4] CICECO-Aveiro Institute of Materials and Department of Materials and Ceramic Engineering, University of Aveiro, 3810-193 Aveiro, Portugal
[5] Smallmatek—Small Materials and Technologies, Lda., Rua Canhas, 3810-075 Aveiro, Portugal
[6] IPMA - Portuguese Institute for the Ocean and Atmosphere, EPPO - Aquaculture Research Station - Av. Parque Natural da Ria Formosa s/n, 8700-194 Olhão, Portugal
[7] Faculty of Sciences & CESAM, University of Lisbon, Campo Grande, 1749-016 Lisbon, Portugal
*Correspondence author: ana.luisa.silva@ua.pt

Abstract

Microplastics and nanomaterials are applied in a myriad of commercial and industrial applications. When leaked to natural environments, such small particles might threaten living organisms' health, particularly when considering their potential combination that remains poorly investigated. This study investigated the physiological and biochemical effects of polyethylene (PE; 64-125 μm in size, 0.1, 1.0, and 10.0 mg.L^{-1}) single and combined with an engineered nanomaterial applied in antifouling coatings, the copper-aluminium layered double hydroxides (Cu-Al LDH; 0.33, 1.0, and 3.33 mg.L^{-1}) in the flatfish *Solea senegalensis* larvae (8 dph) after 3h exposure, in a full factorial design. Particles ingestion, histopathology, and biochemical biomarkers were assessed.

Fish larvae presented < 1 PE particles in their gut, independently of their concentration in the medium. The histological health index showed minimal pathological alterations at PE combined exposure, with a higher value observed at 1 mg LDH.L^{-1} × 0.1 mg PE.L^{-1}. Gut deformity and increased antioxidant defences (catalase), neurotransmission (acetylcholinesterase), and aerobic energy production (electron transport system) were observed at PE ≥ 1.0 mg.L^{-1}. No oxidative damage (lipid peroxidation) or alterations in the detoxification capacity (glutathione-S-transferase) was observed on single and combined exposures. PE, combined or not with Cu-Al LDH, does not seem to compromise larvae' homeostasis considering levels reported so far in the marine and aquaculture environments. However, harsh effects are expected with MP pollution rise, as projections suggest.

Keywords. Cu-Al layered double hydroxides (Cu-Al LDH), nanomaterials, plastic pollution, histopathology, biochemical biomarkers, fish embryotoxicity, co-exposure.

1. Introduction

Microplastics (MPs) pollution is a global issue that threatens marine and coastal environments worldwide. Not surprisingly, the ingestion of significant MPs amounts has been recorded in several marine species from low to high trophic levels, as zooplankton (Beiras et al., 2018), bivalves (Cho et al., 2019), sea turtles (Rizzi et al., 2019), cetaceans (Xiong et al., 2018), and fish (Huang et al., 2020; Naidoo et al. 2020), particularly those collected close to urban coastal areas (Chan et al., 2019). Particles of polyethylene microplastics (PE-MPs), one of the most industrially relevant polymer types, have been found in the guts and intestine of fish from coasts around the world (e.g., McGoran et al., 2018; Chan et al., 2019; James et al., 2020; Barboza et al., 2020; Filgueiras et al., 2020). Since many edible and commercially relevant species present PE (to a greater extent than other MPs) in their gastrointestinal content (Jabeen et al., 2017; Baalkhuyur et al., 2018, 2020; Blettler et al., 2019; Cho et al., 2019; Su et al., 2019; Daniel et al., 2020), their consumption, particularly small-sized animals often consumed as a whole, act as a relevant MPs route for humans, with unpredictable consequences on health (Daniel et al., 2020; Huang et al., 2020; van Raamsdonk et al., 2020).

Under realistic levels, PE-MPs exposure induces physiological, behavioural (e.g., swimming. feeding), biochemical (e.g., neurotoxicity, oxidative stress and damage, impairment on energy acquisition and reserves), and/or developmental changes in fish larvae (e.g., Malafaia et al., 2020; Pannetier et al., 2020; Solomando et al., 2020; Campos et al., 2021). However, contradictory effects due to the PE-MPs ingestion in adult and juvenile fish have been reported, reinforcing that MPs must be considered in programs for monitoring hazard materials in the marine ecosystems (Hamed et al., 2019). While some authors reported that PE-MPs is rapidly expelled without net bioaccumulation and minimal effects (Grigorakis et al., 2017; Ohkubo et al., 2020), others demonstrated that a continuous MPs supply over longer exposure causes adverse effects on growth, reproduction, or survival under (Chisada et al., 2019; Naidoo and

66 Glassom, 2019). In fish early life stages, high levels of PE-MPs (due to high ingestion rates) are
67 known to cause death and decrease larvae density (Steer et al., 2017; Hamed et al., 2019). Such
68 individual effects may impair the population fitness and density in the aquatic environment, thus
69 affecting the food webs by influencing predation (Audzijonyte et al., 2013). Yet, a comprehensive
70 ecotoxicological assessment on fish, particularly in early life stages, regarding PE-MPs in the
71 presence of other contaminants remains scarce in the literature.

72 Moreover, since a wide range of multiple contaminants may occur in the natural
73 environments together with MPs, there is a need to understand the effects caused by their
74 combinations. Notably, the combined effects of MPs with other compounds that present "three-
75 dimensionality" and colloidal behaviour, such as nanoparticles and nanomaterials, remain little
76 explored compared to the combination with chemical compounds (e.g., Polycyclic Aromatic
77 Hydrocarbons and metals). Several engineered nanomaterials (ENMs) have been developed to
78 optimize industrial/commercial production and application of various products, including
79 medical, pharmacological, and nautical products. Among them, the ENM Cu-Al layered double
80 hydroxides (Cu-Al LDH) has been suggested as a promising antifouling nanoadditive for coatings
81 and an adsorbent of chemicals. LDHs are a class of 2D-ENMs, also known as anionic-exchange
82 nanoclays. They present a controlled release capacity and contain outer layers with metal
83 cations (e.g. Zn^{2+}, Cu^{2+}, Al^{3+}) and an interlamellar space stabilized by anions (e.g. NO_3^-) (e.g.,
84 Avelelas et al., 2017; Martins et al., 2017; Kameda et al., 2021). Recent studies highlighted that
85 Zn-Al LDH-NO_3 is low toxic towards marine species (Avelelas et al., 2017; Martins et al., 2017;
86 Gutner-Hoch et al., 2018, 2019). However, Cu-Al LDH-NO_3 effects are not yet reported in the
87 literature. Cu-Al LDH-NO_3 and Cu-Mg-Fe LDH are highly cytotoxic to human stem iPS cells
88 (Kameda et al., 2021) and the freshwater microalgae *Scenedesmus quadricauda* (Ding et al.,
89 2018), respectively, suggesting that Cu-based LDHs may also be deleterious for aquatic biota.
90 From the commercial use, it is expected an increasing frequency of the Cu-Al-NO_3 LDH in the
91 environment, generating environmentally relevant concentrations in the same locations where

there are MPs. The combined effects of PE-MPs and Cu-Al LDH-NO_3 in the marine environment also remain undocumented. However, it is known that environmentally relevant Cu levels, alone or co-exposed with MPs, increase mortality of embryos, inhibit hatching rate, induce oxidative stress and neurotoxicity, and behavioural changes in zebrafish early life stage (Santos et al., 2020a).

Senegal sole, *Solea senegalensis* Kaup, 1858 (order Pleuronectiformes), is a commercially relevant flatfish, natural of Atlantic coasts of Europe and Africa, and farmed in southern European countries (Morais et al., 2014). Because they are demersal and top predators, Sole species are emerging as sentinel fish (e.g., Jebali et al., 2013; Oliva et al., 2013; Cuevas et al., 2015; Briaudeau et al., 2019). Most research focused on juveniles or adults when they are benthic and, thus, susceptible to the effects of sediment contamination (Costa et al., 2009, 2012). However, fish early developmental stages are usually more sensitive to environmental stress and pollution, and the *S. senegalensis* larvae sensitivity to persistent contaminants (Pavlaki et al., 2016; Araújo et al., 2018) makes them suitable for ecotoxicological tests.

This study aimed at assessing the sub-lethal toxicity of PE-MPs and Cu-Al LDH-NO_3, dispersed alone or in combination, towards the flatfish *S. senegalensis* larvae. For that, PE ingestion, histopathological, and biochemical endpoints (lipid peroxidation to infer oxidative damage, electron transport system activity to analyse the aerobic energy consumption, catalase and glutathione-S-transferases activities to assess the antioxidant and detoxification responses, and acetylcholinesterase enzymatic activity as a proxy of the neuromotor activity) were measured. An appropriated chemical characterization of the nanomaterials, and assessing the environmental behaviour and fate of the tested solutions in seawater were evaluated. Our working hypothesis is that tested ENMs will eventually interact with PE-MPs, which might alter their potential bioavailability and toxicity to the flatfish larvae. The ingestion of the particles will likely induce physiological alterations, which may contribute to the increment of reactive oxygen species generation, consequently affecting antioxidant and detoxification capacities, and

impairing neurotransmission. Physiological alterations can also compromise organisms' feeding and swimming behaviour and later result in the loss of energy reserves and impairment in energy acquisition (as reviewed by Jeong and Choi, 2019).

2. Material and methods

2.1 Chemical compounds

Low-density polyethylene (LDPE-MP, CAS 9002-88-4, irregularly shaped, maximum size 125 μm, density 960 kg m^{-3}) were purchased from Sigma-Aldrich UK. The target size range (64 to 125 μm) was obtained by vibratory shaking, and the tested concentrations (0.10, 1.00, 10.00 $mg.L^{-1}$) were prepared as described in Campos et al. (2021). MP size was selected to simulate primary microplastics intentionally included in personal care and hygiene products that are not likely retained by wastewater treatment plants and end up in natural environments at considerable concentrations (Conkle et al., 2017). Such relatively high PE-MPs concentrations were chosen to stimulate larvae to initiate feeding during the relatively short experimental period and infer potential thresholds on feeding behavior and physiological/biochemical endpoints. Notwithstanding, such levels are within the predicted concentrations in aquatic environments (Conkle et al., 2017). Briefly, three concentrated stock solutions (15, 150, and 1500 $mg.L^{-1}$) were prepared in filtered artificial seawater (Tropic Marin Pro Reef salt mixed with reverse osmosis water, practical salinity 35). MP solutions were allowed to age for one week at room temperature, in dark conditions, with continuous shaking (50 rpm). Final MPs concentrations were then obtained by adding 1 mL of the respective solution to each glass test-vial containing 149 mL of the test solution.

Cu-Al layered double hydroxides (Cu-Al LDH-NO_3; hereinafter abbreviated as Cu-Al LDH or LDH) were kindly provided by Smallmatek, Small Materials and Technologies, Lda. According to the procedure described by Martins et al. (2017), these nanomaterials were synthesized through co-precipitation in a Cu/Al proportion of 3:1 and replacing Zn^{2+} with Cu^{2+}. Cu-Al LDH stock

dispersion was prepared with 0.45 µm filtered artificial saltwater and sonicated for 30 min in an ultrasonic bath (Selecta; 40 kHz). Tested concentrations (0.33, 1.00, and 3.33 $mg.L^{-1}$) were chosen based on preliminary acute toxicity studies. They were prepared with 0.45 µm filtered natural seawater (collected from the hatching tanks) through the serial dilutions methodology following the OECD 318 (OECD, 2017).

2.2 Characterization of Cu-Al LDH powders

The morphology and chemical composition of Cu-Al LDH was analyzed by scanning electron microscopy (SEM) Hitachi SU-70 system with an electron beam energy of 15 kV and coupled with energy dispersive spectroscopy (EDS). Cu-Al LDH was structurally and chemically characterized through powder X-Ray Diffraction (XRD) and Fourier transform infrared spectroscopy (FT-IR), respectively. XRD was run at room temperature of the obtained nanomaterial was performed using a PANalytical X'Pert Powder diffractometer (Cu $K\alpha_1$ radiation, λ = 0.154056 nm; 45 kV and 40 mA) coupled with a $PIXcel^{1D}$ detector, and with a step of 0.02° over an angular range (2 Θ) between 4° and 65°. Fourier transform infrared spectroscopy (FT-IR) spectrum was collected in a Perkin Elmer spectrometer Spectrum Two with a UATR TWO unit (Diamond), 64 scans, 4 cm^{-1} resolution, in a wavelength range of 400-4000 cm^{-1}.

2.3 Exposure testing

2.3.1 Test organism

The flatfish *S. senegalensis* larvae of 8 days post-hatching (dph) were obtained from the breeders' natural spawns at the Olhão Pilot Fish Farming Station of the Portuguese Institute of Sea and Atmosphere (IPMA-EPPO) in Algarve, South Portugal. Before transference to experimental vials, larvae were reared in a 1500 L fibreglass tank, with treated natural seawater (i.e., filtrated with a sand filter and a 100 µm cartridge filter, followed by ultra-violet radiation treatment), according to established EPPO protocols (Candeias-Mendes et al., 2013).

167 *2.3.2 Experimental design*

168 Exposure tests were performed in the EPPO facilities to minimize animal stress due to
169 transportation. Experiments included five replicates (each one with 20 larvae), comprised of a
170 control group (only filtered natural seawater), three concentrations of Cu-Al LDH (0.33, 1.00,
171 and 3.33 $mg.L^{-1}$), three concentrations of PE (0.10, 1.00, and 10.00 $mg.L^{-1}$), plus the 9 possible
172 combinations of both PE and LDH treatments arranged in a full factorial design. Organisms were
173 placed in glasses vials containing 150 mL of previously prepared treatments' medium. The
174 experiment ran in the absence of food items (which, at 8 dph, consists of live rotifers and
175 *Artemia* metanauplii ingested *ad libitum*; and usually does not exceed 2-4 h) to stimulate MP
176 ingestion on fish pre-metamorphosis. As *S. senegalensis* fish larvae have a tremendous growth
177 potential per day (Navarro-Guillén et al., 2018), it was intended to guarantee that all exposed
178 organisms presented similar growth stage to accurately relate the responses to exposure
179 conditions and avoid the potential confounding factor caused by the natural variability of larval
180 growth or physiological response to starvation that could be achieved at longer exposure
181 periods. For these reasons, the exposure period was set for 3 h. After this period, each sample
182 composed of the flatfish larvae whole body were immediately preserved according to the
183 endpoint: immersed in 96 % ethanol for PE ingestion analysis (n = 4); frozen in liquid nitrogen in
184 separated microtubes for biochemical biomarkers (n = 10), or immersed in fixative solution for
185 histology (n = 1). The remaining fish larvae (n = 5) were stored at -80 ^{o}C as a potential backup for
186 biochemical or ingestion analysis. Water quality parameters (temperature, conductivity,
187 dissolved oxygen content, and pH) were measured at the end of the exposure.

188 *2.4 Environmental fate and behaviour of tested materials*

189 Exposure conditions were characterized in terms of the tested materials' fate and behaviour
190 (Cu-Al LDHs: single and combined with PE MPs) in the same test media and conditions. A
191 Zetasizer Nano-ZS (Malvern Instruments, UK) was used to perform dynamic light scattering

192 (DLS). For each sample, three measurements were performed. Before the measurements, each
193 sample was placed in an ultrasonic bath (Selecta; 40 kHz; 5 min). The suspensions' average
194 hydrodynamic size was then calculated using the peak 1 (intensity distribution) values.
195 The detailed morphology of both materials following a common dispersion was also analysed
196 by SEM aimed at inspecting if nanoclays were adhered to the PE MPs surface. The worst
197 exposure scenario (PE MP, XX $mg.L^{-1}$ and Cu-Al LDHs, 3.33 $mg.L^{-1}$) was therefore mimicked in a
198 saltwater dispersion that was left 3 h for gentle agitation. The dispersion (volume of 1L) was
199 then filtrated in XX, dried overnight, prepared, and inspected by SEM using a Hitachi SU-70.

200 *2.5 Ecotoxicological endpoints*

201 *2.5.1. Quantification of PE-MPs in the larval gut*

202 All fish larvae were rinsed with ultra-pure water and observed under the stereomicroscope
203 to exclude PE-MPs adhered to their skin. The PE-MPs extraction and quantification followed the
204 optimized protocol developed by Campos et al. (2021). Briefly, to assess the presence of PE-MPs
205 inside organisms, larvae were placed in glass flasks, covered with aluminium foil, dried (50◦C, 24
206 h), digested (HNO_3, 65%; 3 mL; 60°C, 3 h), added hydrogen peroxide (H_2O_2, 35%; 2.6 mL) after
207 cooling down to room temperature, and incubated overnight. Then, samples were diluted (Milli-
208 Q ultra-pure water, 50 mL) and immediately vacuumed filtered onto black polycarbonate filters
209 (PCTE, 0.2 µm pore size, 42 mm Ø, ref. 7063–4702, Cytiva WhatmanTM, Fisher Scientific,
210 Portugal) to retain PE-MPs. MPs were stained with Nile red (1 mL, 5 min, dark; Sigma Aldrich, St.
211 Louis, MO, USA; stock solution: 0.01 $mg.mL^{-1}$ ethanol absolute). After that, filters were washed
212 (ultrapure water) to remove the excess dye and stored in glass Petri-dishes. After drying,
213 polycarbonate filters of each sample were photographed (Canon 550D, EF-S 18–55 mm, Oita,
214 Japan) under a blue light (450 nm, SPEX Forensics, USA) in a dark room using an orange filter
215 (Standard ProMaster®), and the number of MPs was counted. Quality criteria and quality control
216 measures on MPs analysis were taken. Glassware (thoroughly acid-washed and rinsed with Milli-

Q ultrapure water) was preferential for testing and analysis; samples processing was performed in a clean laminar chamber and covered with aluminium foil to avoid airborne contamination. Blanks (1 every 5 samples) were prepared to address possible cross-contamination between samples.

2.5.2. Histopathology

The whole flatfish larvae were fixed (Davidson's solution, 24 h) and then stored in 70 % ethanol. Each sample was pre-embedded in 1 % agarose in distilled water (dH2O) (Tsao-Wu et al., 1998) placed in a horizontal position at the bottom of the wells of a 21-wells silicone mould (250 µL volume). The fish agarose blocks within the cassettes were dehydrated in an increasing series of ethanol (80, 95, and 100 %) and impregnated with paraffin (58 – 60°C) using a protocol adapted from Sabaliauskas et al. (2006) and Copper et al. (2018). The 5 µm thick cross-sections were obtained on a rotary microtome. Slides were stained using regressive Harris hematoxylin and eosin (H&E) and coverslipped with DPX mounting medium for permanent mounting. Photomicrographs of stained sections were taken with a digital camera (Dino-Eye Eyepiece Camera) coupled with an optical light microscope.

The histology-based health status at different levels was defined by the authors adapting the protocols by Bernet et al. (1999), Gusmão et al. (2012), and Cuevas et al. (2015), aiming to score the damages in a semi-quantitative histopathological index level. This histopathological approach considers the relative biological importance (weight) and the dissemination degree (score) of each lesion per organ. The lesions were classified into five reaction patterns: circulatory disturbances, regressive changes (implying functional loss), progressive changes (involving altered function), inflammatory responses, and tumours (Table 1).

The total histopathological index (Ih) was calculated for each individual and organ, according to Cuevas et al. (2015), according to the equation (1):

$$Ih = \sum_1^j w_j a_{jh} \quad (1)$$

where w_j is the weight of the *j* histopathological trait and *aj* the score for the *j* alteration of the *h* individual. The score (*a*), from 0 to 6, depends on the degree and extent of the alteration: 0 = feature/alteration not observed; 2 = mild occurrence; 4 = moderate occurrence; and 6 = severe occurrence (diffuse lesion). Intermediate values were also considered (Bernet et al., 1999).

2.5.3. Biochemical biomarkers

Samples were analysed in terms of lipid peroxidation (LPO) to infer oxidative damage, electron transport system (ETS) activity to analyse the aerobic energy consumption, catalase (CAT) and glutathione-*S*-transferases (GST) activities to assess the antioxidant and detoxification responses, and acetylcholinesterase (AChE) as a proxy of the neuromotor activity. AChE enzyme has been characterized in *S. senegalensis*, mostly located in the brain and muscle tissues due to its role in neural synapsis (Solé et al., 2012).

Samples (preserved at -80°C) were allowed to defrost on ice and homogenized in ultra-pure water (1200 µL) with an ultrasonic homogenizer (cooled in ice during the process) until separation (Rodrigues et al., 2020). For LPO determination, 4 % BHT (2,6-Di-tert-butyl-4-methylphenol) in methanol was added to the homogenate aliquot (200 µL), vortexed, and stored (-80°C) for no more than 24 h. For the ETS measurements, a total of 150 µL of buffer solution (0.3 M Tris base; 0.45 % (w/v) Poly Vinyl Pyrrolidone; 459 mM $MgSO_4$; 0.6 % (v/v) Triton X-100 at pH = 8.5) was added to the homogenate sample (200 µL), agitated and centrifuged (1,000 g, 10 min, 4°C). The remaining homogenate sample was diluted in phosphate buffer solution (0.2 M; pH = 7.4), centrifuged (10,000 g, 15 min, 4°C), and the PMS divided into four aliquots for CAT (100 µL), GST (200 µL), AChE (200 µL), and protein quantification (100 µL) and stored (-80°C) no longer than one week, as previously performed by Rodrigues et al. (2020, 2015) and Campos et al. (2016).

Protein content was determined by the Bradford method (Bradford, 1976), using bovine γ-globulin as a standard at 600 nm. For LPO, thiobarbituric acid-reactive substances (TBARS) were

measured at 535 nm, using a molar extinction coefficient (ε) = 1.56×10^5 $M^{-1}.cm^{-1}$ and expressed as nmol of TBARS mg of $protein^{-1}$ (Bird and Draper, 1984). The ETS activity proceeded by adding 8 mM p-iodonitrotetrazolium (INT), and the reaction was quantified at 490 nm over 3 min. The energy consumption rate (expressed as mJ h^{-1} mg of $protein^{-1}$) was calculated using the stoichiometric relationship (2 mmol of INT-formazan formed, 1 mmol of oxygen consumed), and the Lambert-Beer formula considering a ε = 1.59 x 10^4 $M^{-1}.cm^{-1}$ (De Coen and Janssen, 1997; Rodrigues et al., 2016). CAT activity (as µmol min^{-1} mg of $protein^{-1}$) was determined by measuring the decomposition of the substrate H_2O_2 (35%) at 240 nm for 2 min, using ε = 40 $M^{-1}.cm^{-1}$ (Clairborne, 1985). GST activity was determined by assessing GSH conjugation with 1-chloro-2,4-dinitrobenzene (0.0122 g/mL), at 340 nm, every 20 seconds for 5 min using ε = 9.6×10^3 $M^{-1}.cm^{-1}$ (Habig et al., 1974). AChE activity was measured by the reaction initiated adding a mixture of K-phosphate buffer (0.1 M; pH 7.2), 0.075 M acetylthiocholine iodide, and 10 mM 5,5'-dithiobis (2- nitrobenzoic acid), at 414 nm for 5 min and considering a ε = 13.6×10^3 $M^{-1}.cm^{-1}$ (Ellman et al., 1961; Guilhermino et al., 1996). GST and AChE were expressed as nmol min^{-1} mg of $protein^{-1}$. All procedures were adapted to 96-multiwell plates (Rodrigues et al., 2015; Campos et al., 2016), and samples were pipetted in quadruplicate.

2.6 Statistical analysis

Data were tested for normality (Shapiro-Wilk test) and homoscedasticity (Equal Variance test). If passed ($p > 0.05$), statistical differences between the control and treatments and between isolated and combined treatments (e.g., PE1+LDH1 *vs* PE1; PE1+LDH1 *vs* LDH1) were analyzed by a One-Way Analysis of Variance (ANOVA), followed by Duncan's multiple range test, whenever significant differences were observed. When data failed normality or homoscedasticity, even after data transformation (square root), a Kruskal-Wallis ANOVA on Ranks was implemented, followed by a Dunn's test. The significance level was $p < 0.05$. Then,

291 the no observed effect concentration (NOEC) and the lowest observed effect concentration
292 (LOEC) were derived. Statistical tests were performed using SigmaPlot 12 software.

293 ## 3. Results

294 *3.1 Nanomaterial characterization*

295 Cu-Al LDH presented a hexagonal morphology (Fig. 1A) with a size distribution of 1.31 ± 0.27
296 µm and 1.58 ± 0.19 µm in width and length, respectively, which is in agreement with similar
297 LDHs (Martins et al., 2017). The EDS elemental mapping of the Cu-Al LDH sample and the EDS
298 spectral graph confirmed the presence of Cu (13.02 %) and Al (3.77 %) and its theoretical Cu/Al
299 ratio 3:1 (Fig. 1B and 1C).

300 According to the XRD diffractogram (Fig. 2A), LDH particles present low crystallinity, but it is
301 possible to identify its traditional diffraction peaks with 2θ angles equal to 11.7°, 23.6° and 35.6°
302 could be associated with the (003), (006) and (009) reflection planes of the LDH hexagonal
303 structure. The common diffraction peaks (110) and (113) of the hexagonal structure, usually
304 present at ~60°, were not clearly visible, being masked by the high noise presented in the XRD
305 pattern (Salak et al., 2010; Galvão et al., 2016). Other diffraction peaks were also observed,
306 although with a lack of definition and low crystallinity possible related to some salts from LDH
307 precursors like copper hydroxides or nitrates. FT-IR spectrum of Cu-Al LDH (Fig. 2B) exhibited a
308 broad band around 3378 cm^{-1} from the stretching vibrations of the hydroxyl groups of both layer
309 hydroxide moieties and interlayer water and the deformation vibration mode of OH bonds in
310 water molecules at 1634 cm^{-1}. Additionally, bands around 1000-600 cm^{-1} were assigned to the
311 metal-hydroxide group connection (M-OH) and 600-400 cm^{-1} to the metal-oxygen bond (M-O).
312 The symmetric stretch band of N-O link, associated with nitrates, was present at 1346 cm^{-1}.

313 *3.2 Environmental fate and behaviour of tested particles*

DLS results were summarised in Table 2. A polydispersity index above 0.7 was observed in all measurements, therefore not meeting the quality criteria and indicating high heterogeneity. Consequently, the suspended particles' hydrodynamic size was based on the average value (n = 3) of peak 1 (intensity distribution) of each measurement instead of the Z-average value.

Globally, the hydrodynamic size of Cu-Al LDH in seawater decreased from the lowest to the highest exposure concentration, which can be associated with a rise in the suspended particles' sedimentation rate and/or aggregates/agglomerates formed in time. DLS analysis is for particles smaller than 1 µm; therefore, it does not apply to isolated MP solutions, whose size is > 65 µm. In the co-exposure, the hydrodynamic size increased with both particles' growing concentrations except in the lowest PE concentration; however, the suspended particle size was not remarkably large compared with the isolated materials, indicating that their combination may not greatly affect the aggregation/agglomeration of these particles, and/or light dispersion was affected by the presence of the MPs.

SEM images of the filtrated dispersion containing both tested materials (Fig. 3), demonstrate the occurrence of heteroaggregation phenomena evidenced by single and/or aggregates of Cu-Al LDH hexagonal platelets adhered to the PE microplastics surface.

3.3 Ecotoxicity

No lethality was recorded during the exposure period. The physicochemical parameters were stable in all treatments (average ± standard deviation): pH (7.96 ± 0.02), conductivity (54.72 ± 0.03 µS cm^{-1}), dissolved oxygen (74.42 ± 4.35 %) and temperature (19.53 ± 0.11 °C).

3.3.1 Quantification of ingested PE-MPs

Overall, the number of ingested particles was low, i.e., less than 1 per larvae (Table 3). The highest MPs' ingestion was observed at 10.00 mg PE.L^{-1} in all Cu-Al LDH treatments except at 1.00 mg LDH.L^{-1}, where the highest ingestion was observed at 0.100 mg PE.L^{-1}. However, no

338 statistical differences were observed between concentrations within PE or Cu-Al LDH
339 treatments, and no significant interaction was observed between PE and Cu-Al LDH.

340 *3.3.2 Histopathological assessment*

341 The histopathology analyses of the *S. senegalensis* larvae conducted with the whole body are
342 presented in Fig. 5 and Fig. 6. Tested 8 dph larvae have rudimentary gills (pseudobranch)
343 comprised of five filaments in an ongoing chondrogenesis process and well-developed vision
344 and digestive system (Padrós et al., 2011). Therefore, in this study, the target organs with
345 possible histopathological biomarkers responses were liver, kidney, and gut. The liver structure
346 observed in the control organisms was similar to the larvae exposed to the lowest tested
347 concentration of 0.33 mg Cu-Al LDH.L^{-1}.

348 Despite a significant increase ($H = 34.006$, $df = 15$, $p = 0.003$) in the histopathological index
349 observed in the mixture 1.00 mg LDH.L^{-1} X 0.10 mg PE.L^{-1} (Fig. 3A), the flatfish larvae showed few
350 histopathological alterations' types (Fig. 6) and low histopathological index (Fig. 4A), i.e., low
351 relative biological importance and low dissemination degree of each lesion per organ. Single
352 exposure of the organisms to 1.00 and 3.33 mg Cu-Al LDH.L^{-1} showed hepatic and renal
353 hyperaemia and mild hepatocyte vacuolization, respectively (Fig. 6A, 6B, and 6C). In PE single
354 exposure, a mild gastrointestinal dilation was found in fish exposed at low and moderate
355 concentrations (both 0.10 or 1.00 mg PE.L^{-1}), followed by liver hyperaemia in those exposed to
356 10.0 mg PE.L^{-1} (Fig. 6D). Combined treatments caused gastrointestinal space dilation and
357 hyperaemia of the liver tissue, which were more pronounced in fish exposed to moderate and
358 high concentrations (Fig. 6E, 6F, 6G, and 6H). In some cases, the intestinal tract presented
359 deformities due to MPs presence (Fig. 6G). Also, sacciform cells were present, as observed in
360 control larvae (Fig. 6E).

361 *3.3.3. Biochemical assessment*

Globally, Cu-Al LDH exposure caused no significant effects on the measured endpoints (NOEC ≥ 3.33 mg LDH.L^{-1}). Conversely, single PE exposure to concentrations of PE ≥ 1.00 mg.L^{-1} (Fig. 3: yellow and dark green dots) triggered the changes in antioxidant defences (CAT; Fig. 4C, F = 2.889, p = 0.001; LOEC = 1.00 mg PE.L^{-1}; cf. Table 4), neurotransmission (AChE; Fig. 4B, F = 13.879, p < 0,001; LOEC = 1.00 mg PE.L^{-1}, cf. Table 4), and aerobic energy production (ETS; Fig. 4F, H = 64.565, df = 16, p < 0.001; LOEC = 10.00 mg PE.L^{-1}, cf. Table 4), without causing activation of detoxification enzymes (GST; Fig. 4E) or oxidative damage (LPO; Fig. 4D). The effects of PE mostly remained similar in the presence of Cu-Al LDH nanoclays (Fig. 4C, 4B, and 4F). The exceptions were observed in the combination of 0.33 mg LDH.L^{-1} X 1.00 mg PE.L^{-1} which did not significantly altered CAT activity (Fig. 4C), and 1.00 mg LDH.L^{-1} X 1 mg PE.L^{-1}, which significantly increased (H = 64.565, df = 16, p <0.001) ETS (Fig. 4F; cf. Table 4). The co-exposure of 10.00 mg PE.L^{-1} with low and moderate LDH concentrations caused an increase (F = 2.889, p = 0.001) of the CAT activity on *S. senegalensis* larvae (cf. Fig. 4C; Table 4).

4. Discussion

4.1. Effects of PE-MPs as the only stressor

The detection of low amounts of PE-MPs in the flatfish larvae gut confirmed their capacity to ingest PE-MPs. *S. senegalensis* larvae are capable of successful exogenous feeding after 2 dph, and display active hunting behaviour, mouth and anus opened, and eyes fully pigmented at 3 dph (Ribeiro et al., 1999). According to Huuskonen et al. (2020), fish early life stages do not readily possess additive genetic variation that would help them adapt to the increasing pollution, including by MPs, in their natural environment. Fish cannot actively avoid MPs since they are indistinguishable from natural food (Huuskonen et al., 2020). However, some studies already demonstrated an apparently intentional elimination/spitting following the unintentional intake of MPs particles (Mazurais et al., 2015; Grigorakis et al., 2017; Campos et al., 2021). In fact, unintentional intake and spitting behaviour of MPs might be occurring by *S. senegalensis*

larvae due to the low number of PE-MP particles found in their gut, as it was also observed in *Argyrosomus regius* (meagre) 15 dph larvae (Campos et al., 2021). However, the low number of PE-MPs in the gut might be due to the short period of exposure (3h) or, most likely, due to larvae's egestion rates considering that the histopathological index of the gastrointestinal tract was affected by PE-MPS. Thus, the consequent observed effects might not only be related to the small number of microplastics found inside fish larvae after 3 h exposure, but also to the number of particles that were ingested and spit (including the ones that crossed larvae gills during the respiration process) during that time. In fact, PE-MP ingestion seemed to result in physical damages (particularly in the gastrointestinal tract) on *S. senegalensis*, which could be depicted from the histopathological analysis. Intestinal damage is a key MPs effect on fish (Lei et al., 2018; Qiao et al., 2019). Intestinal histological lesions associated with MPs ingestion, including PE, polyvinyl chloride (PVC) and polystyrene (PS), have been previously reported (Pedà et al., 2016; Mak et al., 2019; Qiao et al., 2019). However, MPs adverse physiological effects are closely dependent on their size (Lei et al., 2018) and the number of particles (Silva et al., 2019, 2020) rather than the chemical composition. MPs can be accumulated in the gut or other tissues and negatively affect animal growth (Yu et al., 2018). As a result of their ingestion (although probably followed by spitting due to the low number of these particles in organisms gut), PE-MPs exposure might impair feeding and induce local immunoreaction and inflammatory responses. The imbalance between feeding intake and energy expenditure caused by these responses likely decrease head/body ratios, changes swimming behaviour, induce oxidative stress, DNA damage, and teratogenicity in fish embryos and larvae, and even cause mortality (Mazurais et al., 2015; Pannetier et al., 2020; Malafaia et al., 2020). However, other studies showed that PE ingestion and toxicity on embryos and larvae are dependent on their concentrations, size and shape (Mazurais et al., 2015; Grigorakis et al., 2017; Pannetier et al., 2019; Ohkubo et al., 2020). Some studies demonstrated that microplastics >10 µm in size accumulate in the digestive tracts and are eventually discarded with the faeces (Cole et al. 2011), whether small microplastics (<10 µm)

413 can translocate from the gut cavity to the circulatory system and body tissues (e.g., Zeytin et al.,
414 2020).

415 Current histological findings linked PE ingestion to gastrointestinal dilation, but further
416 studies are still needed to determine if larvae were able to egest the particles, how the rate of
417 egestion might be affected, and if this may cause damage to the tissue inducing an inflammatory
418 response and affect the fish growth and development. The general histological effects caused
419 by PE particles' ingestion were classified as of minimal pathological importance, namely
420 circulatory disturbance (hyperaemia) and a progressive change (hepatocytes vacuolation).
421 Similar effects were also reported in common soles liver collected along the Basque continental
422 shelf (Cuevas et al., 2015) and other fish species exposed to PE-MPs (Rainieri et al., 2018).
423 Ingestion/egestion of MPs by *S. senegalensis* larvae seem to entail additional energetic cost and
424 oxidative stress and affect neurotransmission. Biochemical results demonstrated that exposure
425 to PE-MPs (≥ 1.00 mg $PE.L^{-1}$) increased the antioxidant defences (particularly CAT activity),
426 neuromotor activity (AChE), and aerobic catabolism (ETS activity). So far, the environmental
427 relevant MPs concentrations reported are often below 1.00 mg $MPs.L^{-1}$ (Beiras and
428 Schönemann, 2020), whereas the biochemical responses were observed above that. These
429 effects suggested an increase in the reactive oxygen species (ROS) generation due to the stress
430 provoked by the PE-MPs ingestion/egestion and spiting, coupled with increased
431 neurotransmission impulses (potentially related to MP spitting and peristaltic movements).
432 Concordantly, the aerobic energy consumption increased since the action of antioxidant
433 defences to prevent cells damage or to deal with potential inflammation processes (which also
434 increase ROS) require high energy expenditure. The ROS generation might respond to larvae to
435 chemical stimuli, or a potential mechanical damage/abrasion or proteolytic damage caused by
436 the ingested particles to the epithelial cells of the gut lumen of fish larvae (Campos et al., 2021).
437 Exposure to PE-MPs increased ROS production and induced antioxidant enzymes and oxidative
438 damage in some organs of gilthead seabream, *Sparus aurata* (Solomando et al., 2020). Meagre

larvae *A. regius* (15 dph) exposed to the same concentrations, size and shape of PE-MPs also demonstrated an increased energy consumption (Campos et al., 2021) but revealed inhibition of the CAT activity and decreased neurotransmission and lipid peroxidation at 10 $mg.L^{-1}$. However, in that study, the exposure period was slightly higher (up to 7h; Campos et al., 2021). Perhaps, in a starvation scenario of 7h, which is common in the overnight period, *S. senegalensis* would present higher oxidative stress induced by the presence/ingestion/egestion and spiting PE-MPs. Previous studies also reported the ability of plastics to induce behavioural alterations and neurotransmission impairment in several invertebrates and fish (Lei et al., 2018; Yu et al., 2018; Pannetier et al., 2020; Prüst et al., 2020; Silva et al., 2019, 2020; Campos et al., 2021).

4.2. Effects of Cu-Al LDH as the only stressor

There were no significant effects observed due to Cu-Al LDH exposure. The mild hepatic histopathological alterations at all tested LDH concentrations were of minimal pathological significance. Larvae exposed to 0.33 mg Cu-Al $LDH.L^{-1}$ exhibited liver structure similar to the control, compatible with previous control situation description (Gusmão et al., 2012; Costa et al., 2013), as normal parenchyma with regular hepatocytes arranged in cords and a single layer of cells lining several sinusoids, which is indicative of good glycogen storage (Simpson, 1992).

The effects of stimuli-responsive ENMs, like LDHs, on marine biota are far from being well understood despite recent efforts (e.g., Figueiredo et al., 2019, 2020; Kaczerewska et al., 2020; Santos et al., 2020b; Jesus et al., 2021). On fish, ENMs, in general, can cause mortality, alterations in growth and reproduction, and can lead to behavioural, physiological, histopathological or biochemical changes in different life stages (e.g., Huang et al., 2018; Yang et al., 2019; Figueiredo et al., 2020). Additionally, gills, intestines, and liver are the organs most endangered when organisms are exposed to ENMs (Handy et al., 2011). Exposure to Cu nanoparticles (NPs; 50 $mg.L^{-1}$, particle size < 50 nm) affected survival, body length and mass, and morphology and physiology of epidermis, gills, and liver on three-day-old Siberian sturgeon

464 larvae, *Acipenser baerii* (Ostaszewska et al., 2016). In zebrafish, early life stages (96 h post-
465 fertilization), Cu ($CuSO_4.5H_2O$; 15 $\mu g.L^{-1}$; 60 $\mu g.L^{-1}$; and 125 $\mu g.L^{-1}$) led to oxidative stress,
466 neurotoxicity, and behavioural alterations (Santos et al., 2020a). In the present study, the
467 absence of adverse effects in the flatfish larvae exposed to Cu-Al LDH, in all ecotoxicological
468 endpoints investigated (until 10.00 $mg.L^{-1}$), is in line with the low or no toxicity findings of the
469 sibling Zn-Al LDH in marine invertebrates, used as a low-toxic "smart" (stimuli-responsive)
470 nanocarriers of active molecules, such as anti-fouling biocides or corrosion inhibitors (Avelelas
471 et al., 2017; Martins et al., 2017; Gutner-Hoch et al., 2018, 2019)

472 4.3. Combined effects of PE-MPs and Cu-AL LDH

473 Generaly, results evidenced that co-exposure did not exacerbate the effects observed in the
474 single exposures, particularly PE-MP that was already inducing some physiological and
475 biochemical effects. However, the LOEC for aerobic metabolism and histopathological index
476 decreased (i.e., increased in effects) to low/middle and middle/middle concentrations of PE/Cu-
477 AL LDH co-exposure compared to single exposures, which highlights the potential interaction
478 between both particles, reinforced by the heteroaggregation processes. Such processes
479 highlight the role of microplastics as vectors of nanomaterials, particularly those that tend to be
480 unstable and aggregate in saltwater, such as LDHs (Martins et al., 2017).

481 Interestingly, CAT (antioxidant defence) and AChE (neurotransmission) in such co-exposure
482 treatments had the lower values and LPO (a proxy for oxidative damage) the higher levels (as
483 depicted in table 4, Fig. 3). Pannetier et al. (2019) demonstrated that single PE-MPs exposure
484 did not cause sublethal toxicity in fish larvae; however, MPs with other contaminants induced
485 lethal and sub-lethal effects mainly when such hazardous chemicals are persistent organic
486 compounds with high potential for bioaccumulation (PAHs, PCBs, among others). Similarly,
487 CYP1A was induced when zebrafish were exposed to virgin and B(a)P-spiked PE-MPs (Batel et
488 al., 2020). Studies with other MPs also demonstrated the deleterious effects of the co-exposure

of MPs (e.g., PS and PVC) and other contaminants (e.g. Cu and Zn), and their key role as vectors of contaminants causing an increase of such chemicals in fish tissues (Brennecke et al., 2016; Qiao et al., 2019). We expected that the effects evaluated would be exacerbated in the combinations of the highest concentrations tested, as nanoclays have the potential to heteroagregate with MPs (see figure and thus induce higher physiological and biochemical responses. However, the investigated NMs (i.e., nanoclays) proved to be safe for the larvae 's health, and the slight effects found due to the MPs' presence were not exalted in the co-exposures under test. Interestingly, LOEC of PE-MPs for aerobic energy consumption and histopathological index decreased after combined exposures with LDH, suggesting an interaction of effects that needs further research.

Another aspect of being considered is the short exposure time, presenting preliminary and pioneer co-exposure of MPs and Cu NMs, since to our knowledge, this is the first study on the topic. For future directions, further studies are needed to assess whether the effects are greater in prolonged exposures. Also, it is interesting to measure the accumulation of NMs in the organisms, which may vary in the presence of MMs, which leads to long-term effects on aquatic organisms and, consequently, on human health.

For final considerations, plastics contamination of seas and oceans, estimated as 4-12 million tons/year (Picó and Barceló, 2019), are expected to be intensified due to the massive use of personal protective equipment during the Covid-19 pandemic (Silva et al., 2020), but its interaction with chemical contaminants present in the marine environment remains not understood. Therefore, the ecological effects derived and/or related to MPs contamination may be strengthened, requiring further investigation and continuous biomonitoring, including key biomarkers responses. Our results reinforce the recommendation to improve regulatory frameworks and legislation on the worldwide use of plastics to minimize plastic leakage and pollution, promote a circular economy, ensure sustainable growth, and protect ecosystems (Silva et al., 2020).

5. Conclusions

PE-MPs' exposure effects isolated or combined with Cu-Al LDH nanoclays on *S. senegalensis* larvae were assessed based on PE ingestion, histopathological, and biochemical biomarkers. Larvae demonstrated low frequencies of histopathological lesions, especially in the liver, and few alterations, mainly hyperaemia and hepatocyte vacuolization, considered evidence of mild inflammation, reversible as the exposure ends. A notable deformity in the intestinal tract caused by the PE ingestion, associated or not to the Cu-Al LDH nanoclays, was recorded, but additional experiments are required to conclude if larvae can expel them or not and with or without additional damage. The biochemical biomarkers responses demonstrated the activation of the first line antioxidant defences, the induction of neurotransmission activities, and a rise in aerobic energy production, all attributed as compensatory metabolic effects caused by ROS generation due to the ingestion of PE-MPs (≥ 1.00 $mg.L^{-1}$). The PE effects persisted in the presence of Cu-Al LDH, but the nanoclay alone did not cause significant effects on the measured endpoints, supporting the eco-friendly labelling of this class of ENMs. PE MPs, single or combined with Cu-Al engineered nanoclays, seem not to compromise the flatfish larvae' homeostasis below environmentally relevant concentrations (1.00 mg $PE.L^{-1}$). Nevertheless, the mild effects observed due to the presence of the PE-MPs may severely compromise *S. senegalensis* health in a predicted future scenario of chronic exposure as plastic waste in oceans is expected to increase and be irreversible disseminated at a global scale as one of the consequences of the current COVID-19 pandemic; and the increased application of polymeric materials (plastics) and nanomaterials (nanoclays) in aquaculture infrastructures (pipes, anticorrosive taints, among others).

Author Contributions.

CESAM team:

Lígia M.B.M. Santana: Data curation, Formal Analysis, Investigation, Methodology, Visualization, Validation. Writing - original draft, Writing - review & editing. Andreia C.M. Rodrigues: Investigation, Methodology, Validation, Writing -

review & editing. Diana Campos: Investigation, Methodology, Validation, Writing - review & editing. Joana Figueiredo: Investigation, Methodology. Sara Silva: Investigation, Methodology. Amadeu M.V.M. Soares: Funding acquisition, Resources. Rui J. M. Rocha: Conceptualization, Resources, Supervision, Writing – review & editing. Carlos Gravato: Writing – review & editing. Ana L. Patrício Silva: Conceptualization, Resources, Funding acquisition, Supervision, Validation, Visualization, Writing – review & editing. Roberto Martins: Conceptualization, Investigation, Project administration, Resources, Supervision, Validation, Writing – review & editing.

CICECO team:

Olga Kaczerewska: Investigation, Methodology. Isabel Sousa: Investigation, Methodology, Visualization, Writing – review & editing. João Tedim: Supervision, Writing – review & editing.

Smallmatek team: Frederico Maia: Investigation, Resources, Writing – review & editing.

EPPO team:

Pedro Pousão-Ferreira: Writing – review & editing. Ana Candeias-Mendes: Writing – review & editing. Florbela Soares: Writing – review & editing. Sara Castanho: Writing – review & editing.

External collaborator:

Denis M.S. Abessa: Funding acquisition, Supervision, Writing – review & editing.

Funding. This work was supported by the bilateral project funded by CAPES (Brazilian Coordination for the Improvement of Higher Education Personnel project nº 88887.156404/2017-00; and post-doctoral scholarship grant nº 88887.296172/2018-00) and FCT (Portuguese Foundation for Science and Technology; 4265 DRI/FCT). Thanks are due to CESAM (UIDP/50017/2020+UIDB/50017/2020), and to CICECO-Aveiro Institute of Materials (UIDB/50011/2020 & UIDP/50011/2020), through FCT/MCTES national funds; to the Integrated Program of SR&T D' Smart Valorisation of Endogenous Marine Biological Resources Under a Changing Climate' (Centro-01-0145-FEDER-000018) co-funded by Centro (2020) program, Portugal 2020, European Union, through the European Regional Development Fund; and to the Project DIVERSIAQUA II (Mar2020-P02M01-0656P). Dr. Roberto Martins and Dr. Ana L. Patrício Silva are funded by an FCT research contract (CEECIND/01329/2017 and CEECIND/01366/2018,

567 respectively). Dr. Denis Abessa thanks the National Council for Scientific and Technological
568 Development (CNPq; grant #308533/2018-6) for the financial support.

569 **Acknowledgements.** The authors would like to thank the Pilot Fish Farming Station in Olhão
570 (EPPO) from the Portuguese Institute for Sea and Atmosphere (IPMA), especially to Laura Ribeiro
571 for the reception and assistance at EPPO; and Silvia Pires for the assistance.

572 **Conflicts of Interest.** The authors declare no conflict of interest.

573 **References**

574 Araújo, M. J., Rocha, R. J. M., Soares, A. M. V. M., Benedé, J. L., Chisvert, A., Monteiro, M. S.,
575 2018. Effects of UV filter 4-methylbenzylidene camphor during early development of *Solea*
576 *senegalensis* Kaup, 1858. Sci. Tot. Environ., 628, 1395-1404.
577 https://doi.org/10.1016/j.scitotenv.2018.02.112
578 Audzijonyte, A., Kuparinen, A., Gorton, R., Fulton, E. A., 2013. Ecological consequences of body
579 size decline in harvested fish species: positive feedback loops in trophic interactions amplify
580 human impact. Biol. letters, 9(2), 20121103. https://doi.org/10.1098/rsbl.2012.1103
581 Avelelas, F., Martins, R., Oliveira, T., Maia, F., Malheiro, E., Soares, A. M., ... Tedim, J., 2017.
582 Efficacy and ecotoxicity of novel anti-fouling nanomaterials in target and non-target marine
583 species. Mar. Biotech., 19(2), 164-174. https://doi.org/10.1007/s10126-017-9740-1
584 Baalkhuyur, F. M., Qurban, M. A., Panickan, P., Duarte, C. M., 2020. Microplastics in fishes of
585 commercial and ecological importance from the Western Arabian Gulf. Mar. Pollut. Bull., 152,
586 110920. https://doi.org/10.1016/j.marpolbul.2020.110920
587 Barboza, L. G. A., Lopes, C., Oliveira, P., Bessa, F., Otero, V., Henriques, B., ... Guilhermino, L.,
588 2020. Microplastics in wild fish from North East Atlantic Ocean and its potential for causing
589 neurotoxic effects, lipid oxidative damage, and human health risks associated with ingestion
590 exposure. Sci. Tot. Environ., 717, 134625. https://doi.org/10.1016/j.scitotenv.2019.134625

591 Batel, A., Baumann, L., Carteny, C. C., Cormier, B., Keiter, S. H., Braunbeck, T., 2020. Histological,
592 enzymatic and chemical analyses of the potential effects of differently sized microplastic
593 particles upon long-term ingestion in zebrafish (*Danio rerio*). Mar. Pollut. Bull., 153, 111022.
594 https://doi.org/10.1016/j.marpolbul.2020.111022
595 Beiras, R., Schönemann, A. M., 2020. Currently monitored microplastics pose negligible
596 ecological risk to the global ocean. Scient. Reports, 10(1), 1-9.
597 https://doi.org/10.1038/s41598-020-79304-z
598 Beiras, R., Bellas, J., Cachot, J., Cormier, B., Cousin, X., Engwall, M., ... López-Ibáñez, S., 2018.
599 Ingestion and contact with polyethylene microplastics does not cause acute toxicity on
600 marine zooplankton. J. Hazard. Mat., 360, 452-460.
601 https://doi.org/10.1016/j.jhazmat.2018.07.101
602 Bernet, D., Schmidt, H., Meier, W., Burkhardt-Holm, P., Wahli, T., 1999. Histopathology in fish:
603 proposal for a protocol to assess aquatic pollution. J. Fish dis., 22(1), 25-34.
604 https://doi.org/10.1046/j.1365-2761.1999.00134.x
605 Bird, R. P., Draper, H. H., 1984. Comparative studies on different methods of malonaldehyde
606 determination. Meth. Enzym., 105, 299-305. https://doi.org/10.1016/S0076-6879(84)05038-
607 2
608 Blettler, M. C., Garello, N., Ginon, L., Abrial, E., Espinola, L. A., Wantzen, K. M., 2019. Massive
609 plastic pollution in a mega-river of a developing country: Sediment deposition and ingestion
610 by fish (Prochilodus lineatus). Environ. Pollut., 255, 113348.
611 https://doi.org/10.1016/j.envpol.2019.113348
612 Bradford, M. M., 1976. A rapid and sensitive method for the quantitation of microgram
613 quantities of protein utilising the principle of protein-dye binding. Analyt. Bioch., 72(1-2),
614 248-254. https://doi.org/10.1016/0003-2697(76)90527-3

615 Brennecke, D., Duarte, B., Paiva, F., Caçador, I., Canning-Clode, J., 2016. Microplastics as vector
616 for heavy metal contamination from the marine environment. Est., Coast. Shelf Sci., 178, 189-
617 195. http://dx.doi.org/10.1016/j.ecss.2015.12.003
618 Briaudeau, T., Zorita, I., Cuevas, N., Franco, J., Marigómez, I., Izagirre, U., 2019. Multi-annual
619 survey of health status disturbance in the Bilbao estuary (Bay of Biscay) based on sediment
620 chemistry and juvenile sole (*Solea* spp.) histopathology. Mar. Pollut. Bull., 145, 126-137.
621 https://doi.org/10.1016/j.marpolbul.2019.05.034
622 Campos, D., Gravato, C., Quintaneiro, C., Soares, A. M.,Pestana, J. L., 2016. Responses of the
623 aquatic midge *Chironomus riparius* to DEET exposure. Aquat. Toxicol., 172, 80-85.
624 https://doi.org/10.1016/j.aquatox.2015.12.020
625 Campos, D., Rodrigues, A., Rocha, R. J., Martins, R., Candeias-Mendes, A., Castanho, S., ...
626 Patrício Silva, A. L., 2021. Are microplastics impairing marine fish larviculture? Preliminary
627 results with *Argyrosomus regius*. Water, 13(1), 104. https://doi.org/10.3390/w13010104
628 Candeias-Mendes, A., Castanho, S., Gamboa, M., Coutinho, J., Bandarra, N., Conceicao, L. E. C., ...
629 Pousão-Ferreira, P., 2013. Advances in larval rearing protocols of sole, *Solea senegalensis*.
630 Commun. Agric. Appl. Biol. Sci., 78(4), 271-274. PMID: 25141688
631 Chan, H. S. H., Dingle, C., Not, C., 2019. Evidence for non-selective ingestion of microplastic in
632 demersal fish. Mar. Pollut. Bull., 149, 110523.
633 https://doi.org/10.1016/j.marpolbul.2019.110523
634 Chisada, S., Yoshida, M., Karita, K., 2019. Ingestion of polyethylene microbeads affects the
635 growth and reproduction of medaka, *Oryzias latipes*. Environ. Pollut., 254, 113094.
636 https://doi.org/10.1016/j.envpol.2019.113094
637 Cho, Y., Shim, W. J., Jang, M., Han, G. M., Hong, S. H., 2019. Abundance and characteristics of
638 microplastics in market bivalves from South Korea. Environ. Pollut., 245, 1107-1116.
639 https://doi.org/10.1016/j.envpol.2018.11.091

640 Clairborne, A., 1985. Catalase activity. In: Greenwald, R.A.E. (Ed.), Handbookof Methods for
641 Oxygen Radical Research. CRC Press, Boca Raton, pp. 283–284.
642 Cole, M., Lindeque, P., Halsband, C., Galloway, TS., 2011. Microplastics as contaminants in the
643 marine environment: A review. Mar Pollut Bull 62:2588–2597.
644 doi:10.1016/j.marpolbul.2011.09.025.
645 Conkle, J. L., Del Valle, C. D. B., Turner, J. W., 2018. Are we underestimating microplastic
646 contamination in aquatic environments?. Environ. Manag., 61(1), 1-8.
647 https://doi.org/10.1007/s00267-017-0947-8
648 Copper, J. E., Budgeon, L. R., Foutz, C. A., van Rossum, D. B., Vanselow, D. J., Hubley, M. J., ...
649 Cheng, K. C., 2018. Comparative analysis of fixation and embedding techniques for optimized
650 histological preparation of zebrafish. Comp. biochem. physiol. C. Toxicol. pharmacol., 208,
651 38-46. https://doi.org/10.1016/j.cbpc.2017.11.003
652 Costa, P. M., Caeiro, S., Costa, M. H., 2013. Multi-organ histological observations on juvenile
653 Senegalese soles exposed to low concentrations of waterborne cadmium. Fish Physiol.
654 Biochem., 39(2), 143-158. https://doi.org/10.1007/s10695-012-9686-1
655 Costa, P. M., Caeiro, S., Vale, C., DelValls, T. À., Costa, M. H., 2012. Can the integration of multiple
656 biomarkers and sediment geochemistry aid solving the complexity of sediment risk
657 assessment? A case study with a benthic fish. Environ. Pollut., 161, 107-120.
658 https://doi.org/10.1016/j.envpol.2011.10.010
659 Costa, P. M., Diniz, M. S., Caeiro, S., Lobo, J., Martins, M., Ferreira, A. M., ... Costa, M. H., 2009.
660 Histological biomarkers in liver and gills of juvenile *Solea senegalensis* exposed to
661 contaminated estuarine sediments: a weighted indices approach. Aquat. toxicol., 92(3), 202-
662 212. https://doi.org/10.1016/j.aquatox.2008.12.009
663 Cuevas, N., Zorita, I., Costa, P. M., Larreta, J., Franco, J. 2015. Histopathological baseline levels
664 and confounding factors in common sole (*Solea solea*) for marine environmental risk

665 assessment. Mar. Environ. Res., 110, 162-173.
666 https://doi.org/10.1016/j.marenvres.2015.09.002
667 Daniel, D. B., Ashraf, P. M., Thomas, S. N., 2020. Microplastics in the edible and inedible tissues
668 of pelagic fishes sold for human consumption in Kerala, India. Environ. Pollut., 266, 115365.
669 https://doi.org/10.1016/j.envpol.2020.115365
670 De Coen, W. M., Janssen, C. R., 1997. The use of biomarkers in Daphnia magna toxicity testing.
671 IV. Cellular energy allocation: a new methodology to assess the energy budget of toxicant-
672 stressed Daphnia populations. J. Aquat. Ecosyst. Stress Recovery, 6(1), 43-55.
673 https://doi.org/10.1023/A:1008228517955
674 Ding, T., Lin, K., Chen, J., Hu, Q., Yang, B., Li, J., Gan, J., 2018. Causes and mechanisms on the
675 toxicity of layered double hydroxide (LDH) to green algae *Scenedesmus quadricauda*. Sci. Tot.
676 Environ., 635, 1004-1011. https://doi.org/10.1016/j.scitotenv.2018.04.222
677 Ellman, G. L., Courtney, K. D., Andres Jr, V., Featherstone, R. M., 1961. A new and rapid
678 colorimetric determination of acetylcholinesterase activity. Biochem. Pharmacol., 7(2), 88-
679 95. https://doi.org/10.1016/0006-2952(61)90145-9
680 Figueiredo, J., Loureiro, S., Martins, R., 2020. Hazard of novel anti-fouling nanomaterials and
681 biocides DCOIT and silver to marine organisms. Environ. Sci. Nano, 7(6), 1670-1680.
682 https://doi.org/10.1039/D0EN00023J
683 Figueiredo, J., Oliveira, T., Ferreira, V., Sushkova, A., Silva, S., Carneiro, D., ... Martins, R., 2019.
684 Toxicity of innovative anti-fouling nano-based solutions to marine species. Environ. Sci. Nano,
685 6(5), 1418-1429. https://doi.org/10.1039/C9EN00011A
686 Filgueiras, A. V., Preciado, I., Cartón, A., Gago, J., 2020. Microplastic ingestion by pelagic and
687 benthic fish and diet composition: A case study in the NW Iberian shelf. Mar. Pollut. Bull.,
688 160, 111623. https://doi.org/10.1016/j.marpolbul.2020.111623
689 Galvão, T. L., Neves, C. S., Caetano, A. P., Maia, F., Mata, D., Malheiro, E., ... Ferreira, M. G.,
690 2016. Control of crystallite and particle size in the synthesis of layered double hydroxides:

691 Macromolecular insights and a complementary modeling tool. J. Colloid Interface Sci., 468,
692 86-94. http://dx.doi.org/10.1016/j.jcis.2016.01.038
693 Grigorakis, S., Mason, S. A., Drouillard, K. G., 2017. Determination of the gut retention of plastic
694 microbeads and microfibers in goldfish (*Carassius auratus*). Chemosphere, 169, 233-238.
695 http://dx.doi.org/10.1016/j.chemosphere.2016.11.055
696 Guilhermino, L., Lopes, M. C., Carvalho, A. P., Soares, A. M. V. M., 1996. Acetylcholinesterase
697 activity in juveniles of *Daphnia magna* Straus. Bull. Environ. Contam. Toxicol., 57(6), 979-985.
698 https://doi.org/10.1007/s001289900286
699 Gusmão, E. P., Rodrigues, R. V., Moreira, C. B., Romano, L. A., Sampaio, L. A., Miranda-Filho, K.
700 C., 2012. Growth and histopathological effects of chronic exposition of marine pejerrey
701 Odontesthes argentinensis larvae to petroleum water-soluble fraction (WSF). Ambio, 41(5),
702 456-466. https://doi.org/10.1007/s13280-012-0259-4
703 Gutner-Hoch, E., Martins, R., Maia, F., Oliveira, T., Shpigel, M., Weis, M., ... Benayahu, Y., 2019.
704 Toxicity of engineered micro-and nanomaterials with antifouling properties to the brine
705 shrimp Artemia salina and embryonic stages of the sea urchin *Paracentrotus lividus*. Environ.
706 Pollut., 251, 530-537. https://doi.org/10.1016/j.envpol.2019.05.031
707 Gutner-Hoch, E., Martins, R., Oliveira, T., Maia, F., Soares, A. M., Loureiro, S., ... Benayahu, Y.,
708 2018. Antimacrofouling efficacy of innovative inorganic nanomaterials loaded with booster
709 biocides. J. Mar. Sci. Eng., 6(1), 6. https://doi.org/10.3390/jmse6010006
710 Habig, W. H., Pabst, M. J., Jakoby, W. B., 1974. Glutathione S-transferases the first enzymatic
711 step in mercapturic acid formation. J. Biol. Chem., 249(22), 7130-7139.
712 https://doi.org/10.1016/S0021-9258(19)42083-8
713 Hamed, M., Soliman, H. A., Osman, A. G., Sayed, A. E. D. H., 2019. Assessment the effect of
714 exposure to microplastics in Nile Tilapia (*Oreochromis niloticus*) early juvenile: I. blood
715 biomarkers. Chemosphere, 228, 345-350.
716 https://doi.org/10.1016/j.chemosphere.2019.04.153

717 Handy, R. D., Al-Bairuty, G., Al-Jubory, A., Ramsden, C. S., Boyle, D., Shaw, B. J., Henry, T. B.,
718 2011. Effects of manufactured nanomaterials on fishes: a target organ and body systems
719 physiology approach. J. Fish Biol., 79(4), 821-853. https://doi.org/10.1111/j.1095-
720 8649.2011.03080.x
721 Huang, J. S., Koongolla, J. B., Li, H. X., Lin, L., Pan, Y. F., Liu, S., ... Xu, X. R., 2020. Microplastic
722 accumulation in fish from Zhanjiang mangrove wetland, South China. Sci. Total Environ., 708,
723 134839. https://doi.org/10.1016/j.scitotenv.2019.134839
724 Huuskonen, H., i Folguera, J. S., Kortet, R., Akkanen, J., Vainikka, A., Janhunen, M., Kekäläinen,
725 J., 2020. Do whitefish (*Coregonus lavaretus*) larvae show adaptive variation in the avoidance
726 of microplastic ingestion?. Environ. Pollut., 262, 114353.
727 https://doi.org/10.1016/j.envpol.2020.114353
728 Jabeen, K., Su, L., Li, J., Yang, D., Tong, C., Mu, J., Shi, H., 2017. Microplastics and mesoplastics in
729 fish from coastal and fresh waters of China. Environ. Pollut., 221, 141-149.
730 https://doi.org/10.1016/j.envpol.2016.11.055
731 James, K., Vasant, K., Padua, S., Gopinath, V., Abilash, K. S., Jeyabaskaran, R., ... John, S., 2020.
732 An assessment of microplastics in the ecosystem and selected commercially important fishes
733 off Kochi, south eastern Arabian Sea, India. Mar. Pollut. Bull., 154, 111027.
734 https://doi.org/10.1016/j.marpolbul.2020.111027
735 Jebali, J., Sabbagh, M., Banni, M., Kamel, N., Ben-Khedher, S., M'hamdi, N., Boussetta, H., 2013.
736 Multiple biomarkers of pollution effects in Solea solea fish on the Tunisia coastline. Environ.
737 Sci. Pollut. Res., 20(6), 3812-3821. https://doi.org/10.1007/s11356-012-1321-2
738 Jeong J. and Choi J., 2019, Adverse outcome pathways potentially related with hazard
739 identification of microplastics based on toxicity mechanisms. Chemosphere, 231, 249-255.
740 https://doi.org/10.1016/j.chemosphere.2019.05.003

741 Jesus, É. P. S., de Figueirêdo, L. P., Maia, F., Martins, R., Nilin, J., 2021. Acute and chronic effects
742 of innovative antifouling nanostructured biocides on a tropical marine microcrustacean. Mar.
743 Pollut. Bull., 164, 111970. https://doi.org/10.1016/j.marpolbul.2021.111970
744 Kaczerewska, O., Sousa, I., Martins, R., Figueiredo, J., Loureiro, S., Tedim, J., 2020. Gemini
745 surfactant as a template agent for the synthesis of more eco-friendly silica nanocapsules.
746 Appl. Sci., 10(22), 8085. https://doi.org/10.3390/app10228085
747 Kameda, T., Horikoshi, K., Kikuchi, H., Kitagawa, F., Kumagai, S., Saito, Y., ... Yoshioka, T., 2021.
748 Kinetic and equilibrium analyses of lactate adsorption by Cu-Al and Mg-Al layered double
749 hydroxides (Cu-Al LDH and Mg-Al LDH) and Cu-Al and Mg-Al layered double oxides (Cu-Al LDO
750 and Mg-Al LDO). Nano-Struct. Nano-Objects, 25, 100656.
751 https://doi.org/10.1016/j.nanoso.2020.100656
752 Lei, L., Wu, S., Lu, S., Liu, M., Song, Y., Fu, Z., ... He, D., 2018. Microplastic particles cause
753 intestinal damage and other adverse effects in zebrafish Danio rerio and nematode
754 Caenorhabditis elegans. Sci. Tot. Environ., 619, 1-8.
755 https://doi.org/10.1016/j.scitotenv.2017.11.103
756 Mak, C. W., Yeung, K. C. F., Chan, K. M., 2019. Acute toxic effects of polyethylene microplastic
757 on adult zebrafish. Ecotoxicol. Environ. Saf., 182, 109442.
758 https://doi.org/10.1016/j.ecoenv.2019.109442
759 Malafaia, G., de Souza, A. M., Pereira, A. C., Gonçalves, S., da Costa Araújo, A. P., Ribeiro, R. X.,
760 Rocha, T. L., 2020. Developmental toxicity in zebrafish exposed to polyethylene microplastics
761 under static and semi-static aquatic systems. Sci. Tot. Environ., 700, 134867.
762 https://doi.org/10.1016/j.scitotenv.2019.134867
763 Martins, R., Oliveira, T., Santos, C., Kuznetsova, A., Ferreira, V., Avelelas, F., ... Loureiro, S., 2017.
764 Effects of a novel anticorrosion engineered nanomaterial on the bivalve *Ruditapes*
765 *philippinarum*. Environ. Sci. Nano, 4(5), 1064-1076. https://doi.org/10.1039/C6EN00630B

766 Mazurais, D., Ernande, B., Quazuguel, P., Severe, A., Huelvan, C., Madec, L., ... Zambonino-
767 Infante, J., 2015. Evaluation of the impact of polyethylene microbeads ingestion in European
768 sea bass (*Dicentrarchus labrax*) larvae. Mar. Environ. Res., 112, 78-85.
769 http://dx.doi.org/10.1016/j.marenvres.2015.09.009
770 Morais, S., Aragão, C., Cabrita, E., Conceição, L. E., Constenla, M., Costas, B., ... Dinis, M. T., 2016.
771 New developments and biological insights into the farming of *Solea senegalensis* reinforcing
772 its aquaculture potential. Rev. Aquac., 8(3), 227-263. https://doi.org/10.1111/raq.12091
773 Naidoo, T., Glassom, D., 2019. Decreased growth and survival in small juvenile fish, after chronic
774 exposure to environmentally relevant concentrations of microplastic. Mar. Pollut. Bull., 145,
775 254-259. https://doi.org/10.1016/j.marpolbul.2019.02.037
776 Naidoo, T., Thompson, R. C., Rajkaran, A., 2020. Quantification and characterisation of
777 microplastics ingested by selected juvenile fish species associated with mangroves in
778 KwaZulu-Natal, South Africa. Environ. Pollut., 257, 113635.
779 https://doi.org/10.1016/j.envpol.2019.113635
780 Navarro-Guillén, C., Engrola, S., Yúfera, M., 2018. Daily dynamic of digestive processes in
781 Senegalese sole (*Solea senegalensis*) larvae and post-larvae. Aquaculture, 493, 100-106.
782 https://doi.org/10.1016/j.aquaculture.2018.04.048
783 OECD, 2017. Dispersion Stability of Nanomaterials in Simulated Environmental Media. Test
784 Guideline No. 318, 32 pp. https://doi.org/10.1787/9789264284142-en
785 Ohkubo, N., Ito, M., Hano, T., Kono, K., Mochida, K., 2020. Estimation of the uptake and gut
786 retention of microplastics in juvenile marine fish: Mummichogs (*Fundulus heteroclitus*) and
787 red seabreams (Pagrus major). Mar. Pollut. Bull., 160, 111630.
788 https://doi.org/10.1016/j.marpolbul.2020.111630
789 Oliva, M., Vicente-Martorell, J. J., Galindo-Riaño, M. D., Perales, J. A., 2013. Histopathological
790 alterations in Senegal sole, *Solea Senegalensis*, from a polluted Huelva estuary (SW, Spain).
791 Fish Physiol. Biochem., 39(3), 523-545. https://doi.org/10.1007/s10695-012-9717-y

792 Ostaszewska, T., Chojnacki, M., Kamaszewski, M., Sawosz-Chwalibóg, E., 2016. Histopathological
793 effects of silver and copper nanoparticles on the epidermis, gills, and liver of Siberian
794 sturgeon. Environ. Sci. Pollut. Res., 23(2), 1621-1633. https://doi.org/10.1007/s11356-015-
795 5391-9
796 Padrós, F., Villalta, M., Gisbert, E., Estévez, A., 2011. Morphological and histological study of
797 larval development of the Senegal sole *Solea senegalensis*: an integrative study. J. Fish Biol.,
798 79(1), 3-32. https://doi.org/10.1111/j.1095-8649.2011.02942.x
799 Pannetier, P., Morin, B., Clérandeau, C., Laurent, J., Chapelle, C., Cachot, J., 2019. Toxicity
800 assessment of pollutants sorbed on environmental microplastics collected on beaches: Part
801 II-adverse effects on Japanese medaka early life stages. Environ. Pollut., 248, 1098-1107.
802 https://doi.org/10.1016/j.envpol.2018.10.129
803 Pannetier, P., Morin, B., Le Bihanic, F., Dubreil, L., Clérandeau, C., Chouvellon, F., ... Cachot, J.,
804 2020. Environmental samples of microplastics induce significant toxic effects in fish larvae.
805 Environ. Intern., 134, 105047. https://doi.org/10.1016/j.envint.2019.105047
806 Pavlaki, M. D., Araújo, M. J., Cardoso, D. N., Silva, A. R. R., Cruz, A., Mendo, S., ... Loureiro, S.,
807 2016. Ecotoxicity and genotoxicity of cadmium in different marine trophic levels. Environ.
808 Pollut., 215, 203-212. https://doi.org/10.1016/j.envpol.2016.05.010
809 Pedà, C., Caccamo, L., Fossi, M. C., Gai, F., Andaloro, F., Genovese, L., ... Maricchiolo, G., 2016.
810 Intestinal alterations in European sea bass *Dicentrarchus labrax* (Linnaeus, 1758) exposed to
811 microplastics: preliminary results. Environ. Pollut., 212, 251-256.
812 http://dx.doi.org/10.1016/j.envpol.2016.01.083
813 Picó, Y., Barceló, D., 2019. Analysis and prevention of microplastics pollution in water: current
814 perspectives and future directions. ACS omega, 4(4), 6709-6719.
815 https://doi.org/10.1021/acsomega.9b00222
816 Prüst, M., Meijer, J., Westerink, R. H., 2020. The plastic brain: neurotoxicity of micro-and
817 nanoplastics. Part. Fibre Toxicol., 17, 1-16. https://doi.org/10.1186/s12989-020-00358-y

818 Qiao, R., Lu, K., Deng, Y., Ren, H., Zhang, Y., 2019. Combined effects of polystyrene microplastics
819 and natural organic matter on the accumulation and toxicity of copper in zebrafish. Sci. Tot.
820 Environ., 682, 128-137. https://doi.org/10.1016/j.scitotenv.2019.05.163
821 Rainieri, S., Conlledo, N., Larsen, B. K., Granby, K., Barranco, A., 2018. Combined effects of
822 microplastics and chemical contaminants on the organ toxicity of zebrafish (*Danio rerio*).
823 Environ. Res., 162, 135-143. https://doi.org/10.1016/j.envres.2017.12.019
824 Ribeiro, L., Sarasquete, C., Dinis, M. T., 1999. Histological and histochemical development of the
825 digestive system of *Solea senegalensis* (Kaup, 1858) larvae. Aquaculture, 171(3-4), 293-308.
826 https://doi.org/10.1016/S0044-8486(98)00496-7
827 Rizzi, M., Rodrigues, F. L., Medeiros, L., Ortega, I., Rodrigues, L., Monteiro, D. S., Kessler, F.,
828 Proietti, M. C., 2019. Ingestion of plastic marine litter by sea turtles in southern Brazil:
829 abundance, characteristics and potential selectivity. Mar. Pollut. Bull., 140, 536-548.
830 https://doi.org/10.1016/j.marpolbul.2019.01.054
831 Rodrigues, A. C., Gravato, C., Quintaneiro, C., Golovko, O., Žlábek, V., Barata, C., ... Pestana, J.
832 L., 2015. Life history and biochemical effects of chlorantraniliprole on *Chironomus riparius*.
833 Sci. Tot. Environ., 508, 506-513. https://doi.org/10.1016/j.scitotenv.2014.12.021
834 Rodrigues, A. C., Henriques, J. F., Domingues, I., Golovko, O., Žlábek, V., Barata, C., ... Pestana,
835 J. L., 2016. Behavioural responses of freshwater planarians after short-term exposure to the
836 insecticide chlorantraniliprole. Aquat. Toxicol., 170, 371-376.
837 https://doi.org/10.1016/j.aquatox.2015.10.018
838 Rodrigues, A., Gravato, C., Silva, C. J., Pires, S. F., Costa, A. P., Conceição, L. E., ... Rocha, R. J.,
839 2020. Seasonal temperature fluctuations differently affect the immune and biochemical
840 parameters of diploid and triploid oncorhynchus mykiss cage-cultured in temperate
841 latitudes. Sustainability, 12(21), 8785. https://doi.org/10.3390/su12218785

842 Sabaliauskas, N. A., Foutz, C. A., Mest, J. R., Budgeon, L. R., Sidor, A. T., Gershenson, J. A., ...
843 Cheng, K. C., 2006. High-throughput zebrafish histology. Methods, 39(3), 246-254.
844 https://doi.org/10.1016/j.ymeth.2006.03.001
845 Salak, A. N., Tedim, J., Kuznetsova, A. I., Zheludkevich, M. L., Ferreira, M. G. (2010). Anion
846 exchange in Zn–Al layered double hydroxides: in situ X-ray diffraction study. Chem. Phys.
847 Letters, 495(1-3), 73-76. https://doi.org/10.1016/j.cplett.2010.06.041
848 Santos, D., Félix, L., Luzio, A., Parra, S., Cabecinha, E., Bellas, J., Monteiro, S. M., 2020a.
849 Toxicological effects induced on early life stages of zebrafish (*Danio rerio*) after an acute
850 exposure to microplastics alone or co-exposed with copper. Chemosphere, 261, 127748.
851 https://doi.org/10.1016/j.chemosphere.2020.127748
852 Santos, J. V. N. D., Martins, R., Fontes, M. K., Campos, B. G. D., Maia, F., Abessa, D. M. D. S.,
853 Perina, F. C., 2020b. Can encapsulation of the biocide DCOIT affect the anti-fouling efficacy
854 and toxicity on tropical bivalves? Appl. Sci., 10(23), 8579.
855 https://doi.org/10.3390/app10238579
856 Silva, M. S. S., Oliveira, M., Valente, P., Figueira, E., Martins, M., Pires, A., 2019. Behavior and
857 biochemical responses of the polychaeta *Hediste diversicolor* to polystyrene nanoplastics. Sci.
858 Tot. Environ., 707, 134434. https://doi.org/10.1016/j.scitotenv.2019.134434
859 Silva, A. L. P., Prata, J. C., Walker, T. R., Duarte, A. C., Ouyang, W., Barcelò, D., Rocha-Santos, T.,
860 2020. Increased plastic pollution due to COVID-19 pandemic: Challenges and
861 recommendations. Chem. Eng. J., 126683.
862 https://doi.org/10.1016/j.cej.2020.126683Simpson, M. G., 1992. Histopathological changes
863 in the liver of dab (*Limanda limanda*) from a contamination gradient in the North Sea. Mar.
864 Environ. Res., 34(1-4), 39-43. https://doi.org/10.1016/0141-1136(92)90080-6
865 Solé, M., Vega, S., Varó, I., 2012. Characterization of type “B” esterases and hepatic CYP450
866 isoenzimes in Senegalese sole for their further application in monitoring studies. Ecotoxicol.
867 Environ. Saf., 78, 72-79. https://doi.org/10.1016/j.ecoenv.2011.11.013

Solomando, A., Capó, X., Alomar, C., Álvarez, E., Montserrat, C., Valencia, J.M., Pinya, S., Deudero, S., Sureda, A., 2020. Long-term exposure to microplastics induces oxidative stress and a pro-inflammatory response in the gut of *Sparus aurata* Linnaeus, 1758. Environ. Pollut. 266, 115295. https://doi.org/10.1016/j.envpol.2020.115295

Steer, M., Cole, M., Thompson, R. C., Lindeque, P. K., 2017. Microplastic ingestion in fish larvae in the western English Channel. Environ. Pollut., 226, 250-259. http://dx.doi.org/10.1016/j.envpol.2017.03.062

Su, L., Deng, H., Li, B., Chen, Q., Pettigrove, V., Wu, C., Shi, H., 2019. The occurrence of microplastic in specific organs in commercially caught fishes from coast and estuary area of east China. J. Hazard. Mat., 365, 716-724. https://doi.org/10.1016/j.jhazmat.2018.11.024

Tsao-Wu, G. S., Weber, C. H., Budgeon, L. R., Cheng, K. C., 1998. Agarose-embedded tissue arrays for histologic and genetic analysis. Biotechniques, 25(4), 614-618. https://doi.org/10.2144/98254st02

van Raamsdonk, L. W., van der Zande, M., Koelmans, A. A., Hoogenboom, R. L., Peters, R. J., Groot, M. J., ... Weesepoel, Y. J., 2020. Current insights into monitoring, bioaccumulation, and potential health effects of microplastics present in the food chain. Foods, 9(1), 72. https://doi.org/10.3390/foods9010072

Xiong, X., Chen, X., Zhang, K., Mei, Z., Hao, Y., Zheng, J., ... Wang, D., 2018. Microplastics in the intestinal tracts of East Asian finless porpoises (*Neophocaena asiaeorientalis sunameri*) from Yellow Sea and Bohai Sea of China. Mar. Pollut. Bull., 136, 55-60. https://doi.org/10.1016/j.marpolbul.2018.09.006

Yang, C. H., Kung, T. A., Chen, P. J., 2019. Differential alteration in reproductive toxicity of medaka fish on exposure to nanoscale zerovalent iron and its oxidation products. Environ. Pollut., 252, 1920-1932. https://doi.org/10.1016/j.envpol.2019.05.154

892 Yu, P., Liu, Z., Wu, D., Chen, M., Lv, W., Zhao, Y., 2018. Accumulation of polystyrene microplastics
893 in juvenile Eriocheir sinensis and oxidative stress effects in the liver. Aquat. Toxicol., 200, 28-
894 36. https://doi.org/10.1016/j.aquatox.2018.04.015
895 Zeytin S., Wagner, G., Mackay-Roberts, N., Gerdts, G., Schuirmann, E., Klockmann, S., Slater, M.,
896 2020, Quantifying microplastics translocation from feed to the fillet in European seabass
897 Bicentrarchus labrax. Mar Pollut Bull. 156, 111210.
898 https://doi.org/10.1016/j.marpolbul.2020.111210
899

Table 1. Histopathological assessment index for fish organs (I_{org}) according to the importance factor (w) of each alteration (*j*) of the reaction pattern (rp) in the respective target organ (org).

Reaction pattern (rp)	Alteration (*j*)	Importance factor (w)
Circulatory disturbances	haemorrhage	1
	hyperaemia	1
	Aneurysm	1
Regressive changes	Deposits	1
	Nuclear alterations	2
	Atrophy	2
	Necrosis	3
Progressive changes	Hypertrophy	1
	Fat vacuolation of hepatocytes*	1
	Hyperplasia	2
inflammatory responses	Melanomacrophage centres	1
	Lymphocytic infiltration	2
Tumour	Tumour	3

Pathological importance: 1 = Minimal (easily reversible as exposure end); 2 = Moderate (mostly reversible if the stressor is neutralised); and 3 = Marked (generally irreversible, leading to a partial or total loss of the organ function). *Specific for hepatic tissue. Adapted from Bernet et al. (1999), Gusmão et al. (2012), and Cuevas et al. (2015)

Table 2. Mean values of the particle size distribution (units: nm; average and standard deviation (SD); n = 3) based on the dynamic light scattering (DLS) analysis of all treatments of Cu-Al LDH (LDH) and polyethylene microplastic (PE) samples dispersed in natural seawater during the exposure testing.

Exposure conditions	Concentration ($mg.L^{-1}$)	Size (mean±SD) (nm)
Control	0	251.7 ± 20.8
LDH1	0.33	383.3 ± 20.8
LDH2	1.00	177.1 ± 28.0
LDH3	3.33	136.3 ± 24.1
PE1/LDH1	0.10/0.33	299.1 ± 8.7
PE1/LDH2	0.10/1.00	393.2 ± 36.4
PE1/LDH3	0.10/3.33	265.3 ± 34.3
PE2/LDH1	1.00/0.33	349.6 ± 29.6
PE2/LDH2	1.00/1.00	335.5 ± 11.3
PE2/LDH3	1.00/3.33	466.1 ± 19.4
PE3/LDH1	10.0/0.33	202.6 ± 4.8
PE3/LDH2	10.0/1.00	336.3 ± 39.8
PE3/LDH3	10.0/3.33	374.7 ± 10.7

911 **Table 3.** Number of ingested polyethylene microplastics (PE; mean ± standard error; n = 5, 4 larvae per replicate) by
912 *Solea senegalensis* larvae 8 dph after 3 h exposure to Cu-Al LDH (LDH) and PE.

LDH (mg.L^{-1}) \ PE (mg.L^{-1})	0.10	1.00	10.00
0.00	0.15 ± 0.06	0.06 ± 0.06	0.38 ± 0.29
0.33	0.06 ± 0.06	0.10 ± 0.06	0.31 ± 0.12
1.00	0.19 ± 0.10	0.06 ± 0.06	0.13 ± 0.07
3.33	0.00 ± 0.00*	0.00 ± 0.00	0.33 ± 0.20

913 * Only 2 of the 5 replicates were considered due to a technical issue.
914

915

916 **Table 4.** NOEC (No Observed Effect Concentration) and LOEC (Lowest Observed Effect Concentration) values of the
917 ecotoxicological assessments of *Solea senegalensis* larvae 8 dph exposed to a full factorial design of polyethylene
918 microplastics (PE) and Cu-Al layered double hydroxides (LDH) nanomaterial. Units are given in mg.L^{-1}.

Exposure	LDH		PE		PE/LDH	
Parameter	NOEC	LOEC	NOEC	LOEC	NOEC	LOEC
CAT	-	-	0.10	1.00	1.00/0.33	1.00/1.00
GST	-	-	-	-	-	-
AChE	-	-	0.10	1.00	0.10/3.33	1.00/0.33
LPO	-	-	-	-	-	-
ETS	-	-	1.00	10.00	1.00/0.33	1.00/1.00
I *value*	-	-	-	-	0.10/0.33	0.10/1.00

919

920
921

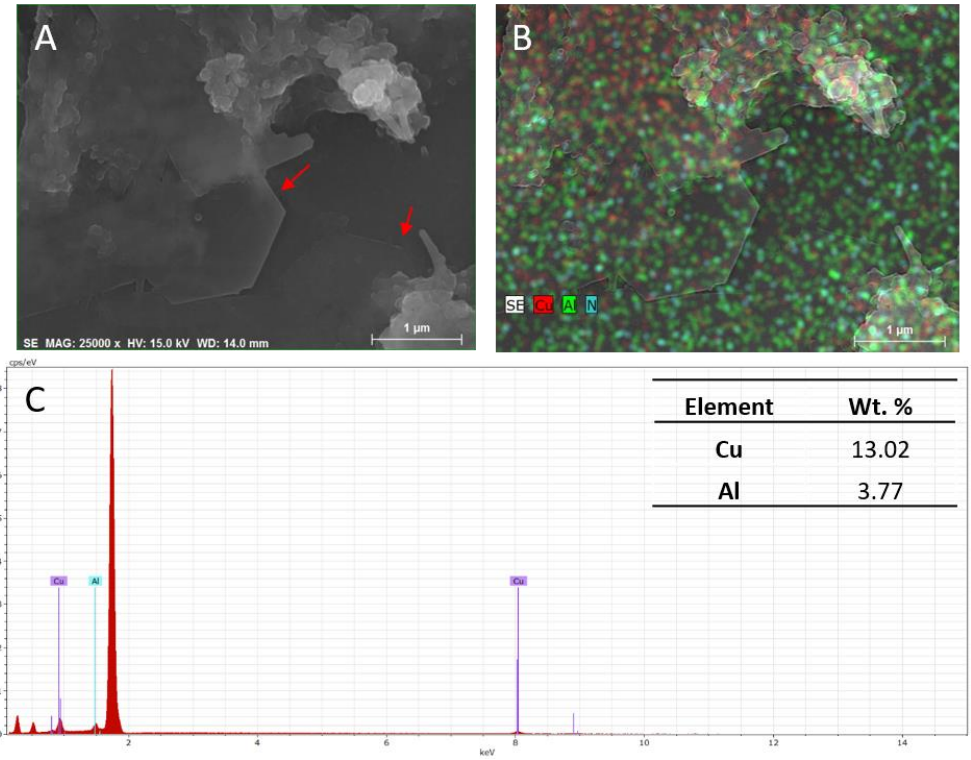

Fig. 1. Morphology and composition of CuAl-LDH. A) Scanning electron microscopy (SEM) image, with red arrows pointing to the hexagonal morphology. B) EDS elemental mapping. C) EDS spectra graph and a summary table of the major elements' proportion.

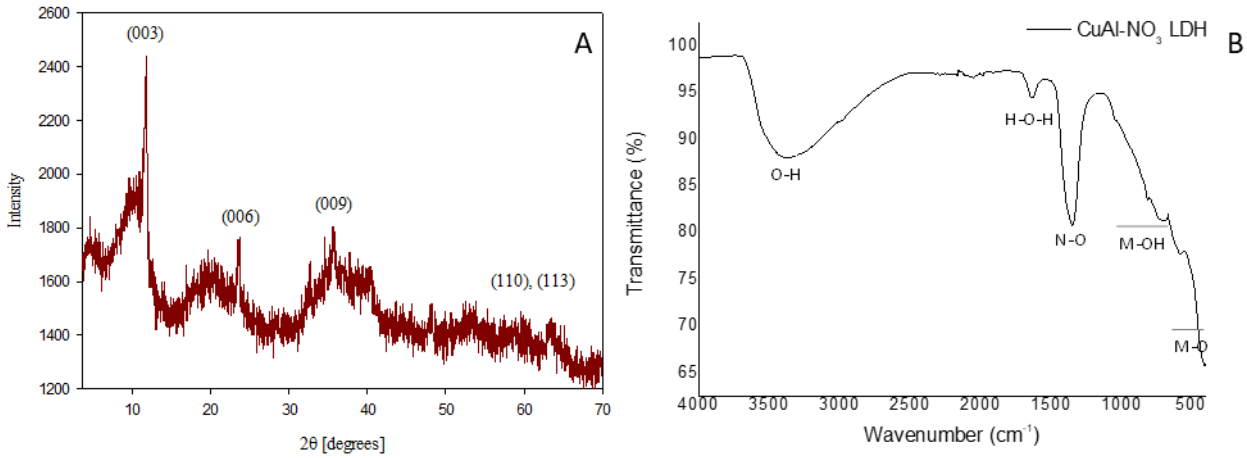

Fig. 2. XRD (A) and FT-IR (B) patterns of Cu-Al LDH.

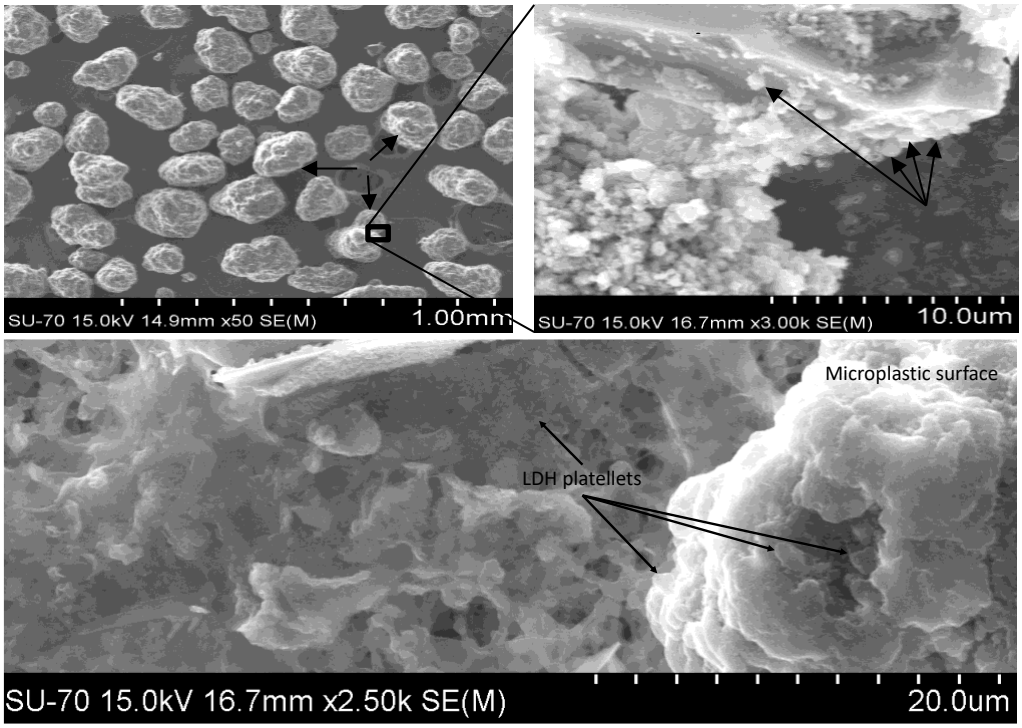

Fig. 3: Morphology of polyethylene (PE) microplastics in the upper left image and its heteroaggregates with the CuAl-LDH nanoclays (both upper right and lower images) obtained by scanning electron microscopy (SEM). Black arrows are pointing to the nanoclays adhered to PE microplastics surface.

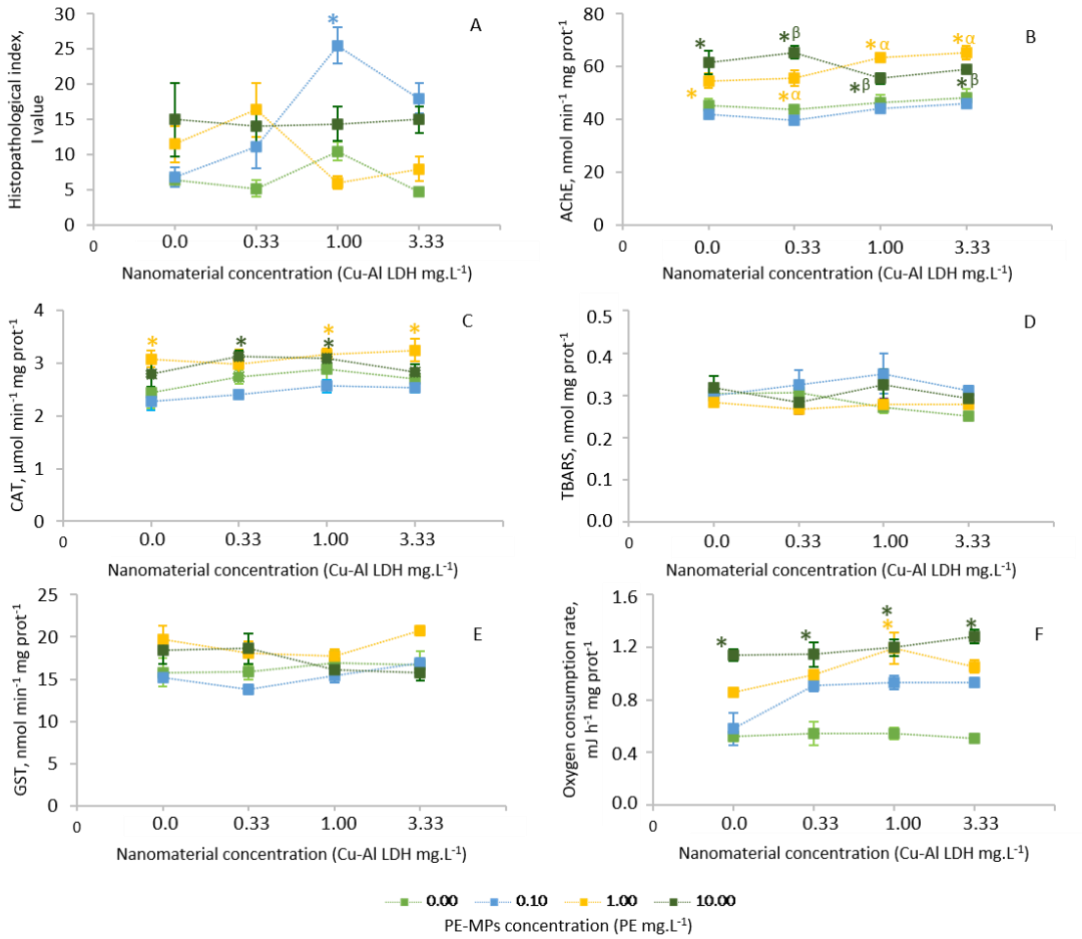

Fig. 4. Histopathological and biochemical assessment of *Solea senegalensis* larva 8 dph (n = 5, and n = 50, respectively) exposed to a full factorial design of polyethylene microplastics (PE) and Cu-Al layered double hydroxides (Cu-Al LDH) nanomaterial. A) Histopathological condition index (I *value*). B) Acetylcholinesterase activity. C) Catalase activity. D) Lipid peroxidation. E) Glutathione S-transferase activity. F) Electron transport system activity. *indicate significant difference from the control group. $^{\alpha}$ indicate significant difference from the correspondent nanomaterial group. $^{\beta}$ indicate significant difference from the correspondent PE group. Significance level ($p < 0.05$). Mean values ± SE.

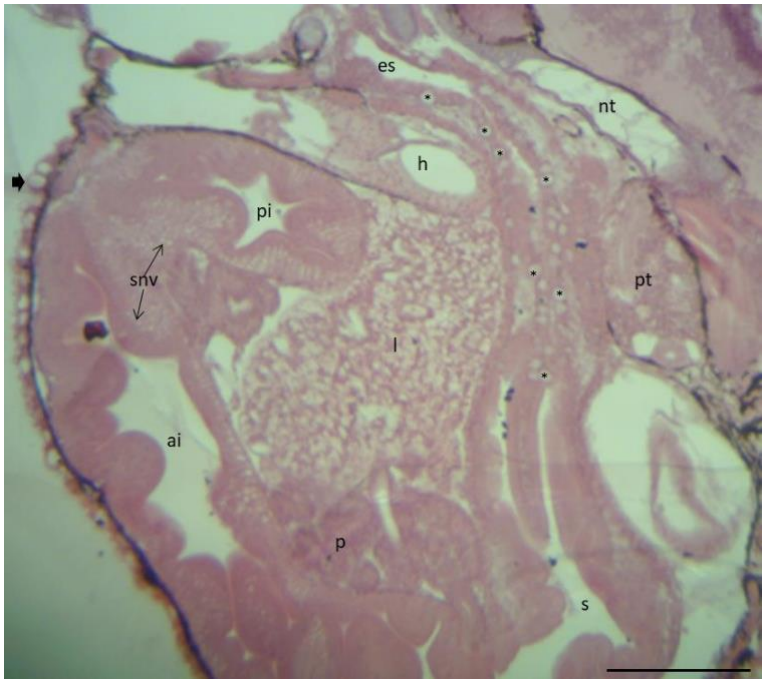

Fig. 5. Photomicrograph of control *Solea senegalensis* larva 8 dph. * thyroid follicles; ➧ sacciform cells; ai, anterior intestine; es, oesophagus; h, heart; l, liver; nt, nothocord; p, pancreas; pi, posterior intestine; pt, pronephric tubule; s, stomach; snv, supranuclear vacuoles. H&E. Scale bar 20 µm.

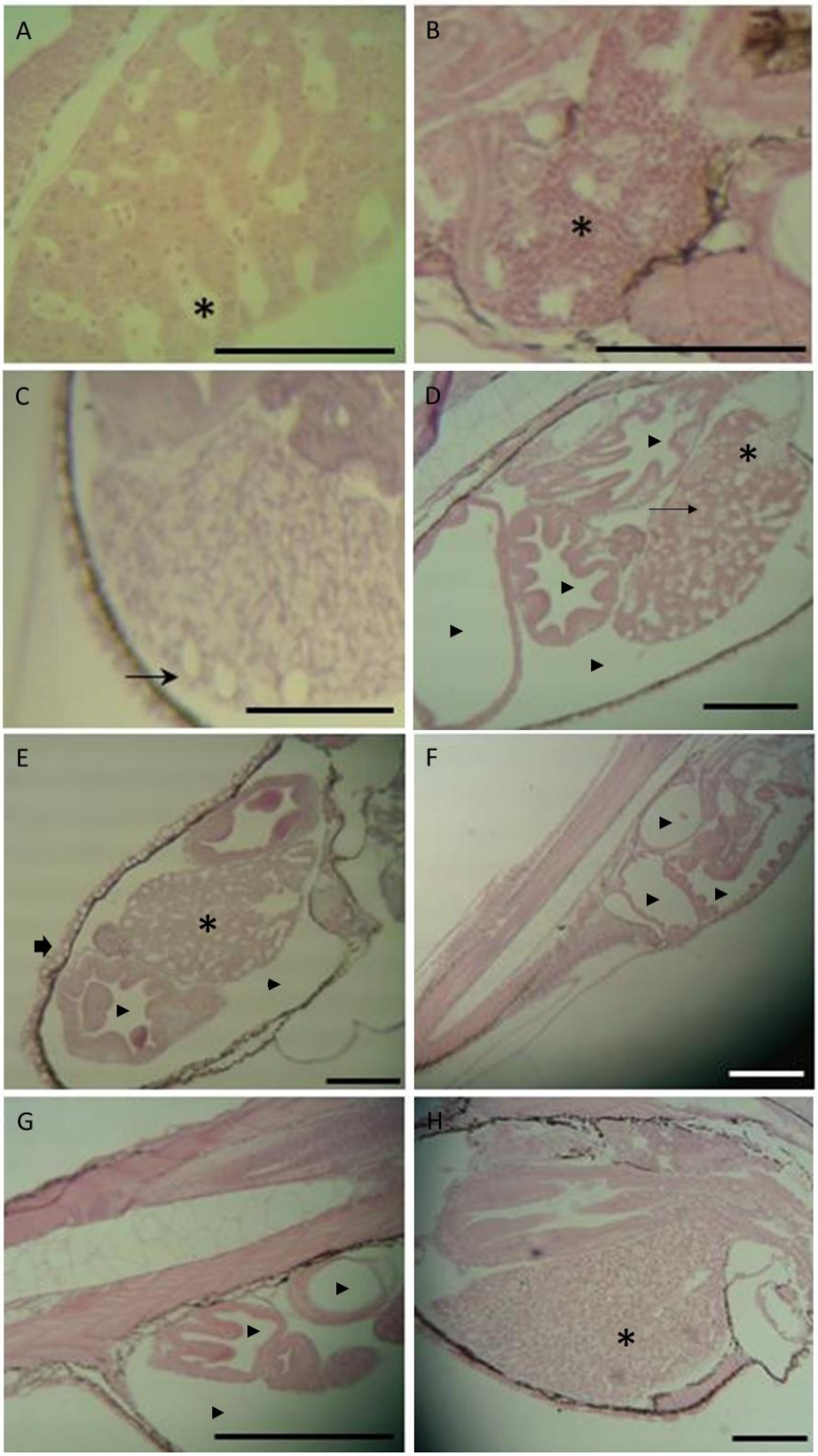

Fig. 6. Photomicrograph of *Solea senegalensis* larva 8 dph. A) Hyperaemia (*) in hepatic tissue at 1.00 mg Cu-Al LDH.L^{-1} exposure. B) Hyperaemia (*) in renal tissue at 1.00 mg Cu-Al LDH.L^{-1} exposure. C) Vacuolation (arrow) of hepatocytes at 3.33 mg Cu-Al LDH.L^{-1}. D) Cellular alterations observed at 10.00 mg PE.L^{-1} exposure, including vacuolation (arrow) of hepatocytes, gastrointestinal dilation (arrowhead) and hyperaemia (*) of liver tissue. E) Hyperaemia (*) and vacuolation of hepatocytes, sacciform cells (large arrow) and gastrointestinal dilation (arrowhead) at 0.10 mg PE.L^{-1} + 3.33 mg Cu-Al LDH.L^{-1}. F) and G) Gastrointestinal dilation (arrowhead) at 1.00 mg PE.L^{-1} + 3.33 mg Cu-Al LDH.L^{-1}. H) Hyperaemia (*) of hepatocytes at 10.00 mg PE.L^{-1} + 1.00 mg Cu-Al LDH.L^{-1}. H&E. Scale bar 20 µm.